On deletion of questionable electron density profiles retrieved using the COSMIC radio occultation (RO) technique

P. S. Brahmanandam[1, *], Y. H. Chu[2], G. Uma[2], and Jens Wickert[3]

1. Madanapalle Institute of Technology and Science, Madanapalle, AP, India
2. Institute of Space Science, Natl. Central University, Chung-Li, Taiwan
3. GFZ German Research Center for Geosciences, Potsdam, Germany.

(dranandpsb@mits.ac.in)*

ABSTRACT

The crucial assumption made in the retrieval of radio-occulted atmospheric parameters based on the Abel transformation is the spherical symmetry of the atmospheric refractive index, which implies that no horizontal gradient of the refractive index exists along the spherical shell. Nevertheless, the presence of density irregularities will lead to scintillation and multipath effects that often create highly fluctuating and random electron density profiles. In this study, it is proposed a reliable approach to remove questionable electron density profiles retrieved using the COSMIC RO technique basing on two parameters, namely, the gradient and fluctuation of the topside density profile. Statistics of seven year density profiles (July 2006 – May 2013) show that, on average, 98% of the electron density profiles have upper electron density gradients and electron density fluctuations smaller than -0.02 #/m3/m and 0.2, respectively, which can be treated as good data for further analysis. Though the percentage of questionable data are too meager (only 2%), global comparisons between density profiles before and after the removal of questionable data have revealed few differences. The computed gradients and fluctuations of the topside ionosphere electron density profiles have shown few important features including solar activity dependency and pronounced variations between around $+40^0$ and -40^0 latitudes. After the removal of questionable profiles, an analysis made between peak densities and heights of the ionosphere F layer during different seasons of years 2007 and 2012 that revealed several important features. The important aspect of our algorithm is that it removes questionable electron density profiles effectively without relying on any model and other observations.

1. INTRODUCTION

The crucial assumptions in GPS RO techniques are that the spherical symmetry of atmosphere refractive at the locality of occultations [*Hajj et al., 2000; Kursinski et al., 2000*] and geometrical optics assumption [*Kursinski et al., 2000*], although the assumption of spherical symmetry is almost never true [*Schreiner, 1999; Yue et al., 2010; Yue et al., 2011b*]. More specifically, spherical symmetry assumption implies that no horizontal gradients of refractive exist along the spherical shell. In fact, it is true that if there are no irregular electron density distributions in the GPS ray path the occultation-retrieved electron density will be a smooth curve without random fluctuations superimposed on the curve. In reality, nonetheless, the presence of ionospheric irregularities is obvious particularly at equatorial, ionization anomaly crest (during local sunset times) and at high-latitude regions even during daytime hours and during space weather events including geo-magnetically disturbed and solar radio burst (SRB) [*Yue et al., 2013*] epochs. As a result, the retrieved electron density profile will be highly fluctuating due to irregular variation in the bending angle of the ray path which eventually gives

rise to a large uncertainty in the estimation and impairment of the data reliability [*Yang et al., 2009; Potula et al., 2011*].

Several GPS RO missions sponsored countries have made serious efforts to relinquish unreliable and questionable density profiles including COSMIC Data Analysis and Archive Center (CDAAC). Although CDAAC in Boulder, USA has implemented 'quality control (QC)' schemes to profoundly reject questionable and unreliable density profiles, it cannot almost delete those profiles that are occurring due to ionosphere irregularities [*Chu et al., 2010; Potula et al., 2011*]. In this research, we propose a more realistic and reliable approach, yet simple, which solely rely on COSMIC retrieved density profiles to remove questionable and unreliable electron densities from the original RO data set. By using mean deviation (MD) of electron density fluctuations and slope (or vertical gradient) of the topside electron density profile, we set up threshold limits to screen-out unreliable and questionable density profiles based on the statistics of seven year (July 2006-May 2013) database.

2. TYPICAL EXAMPLES

Two panels in Figure 1 show electron density profiles measured by same satellite (FM2), which received the GPS signals transmitted from GPS satellite numbers 19 (left panel) and 08 (right panel) respectively, but geographically left (right) electron density profile belongs to southern (northern) hemisphere at -8.05 ^{0}S (2.38^0 N) on 31 May 2007. As shown, both profiles are showing exceedingly irregular fluctuations in the height variations of electron densities. It is, therefore, nearly impossible to retrieve important ionospheric parameters including the peak height of the F2-layer (hmF2), peak density at the F2 layer (NmF2) and others from these profiles, which should ultimately be deleted to avoid their involvement in further processing. Figure 2 depicts few typical examples on electron density profiles that are showing either positive gradient (i.e. electron density increases with increasing height) or near vertical slope at the topside ionosphere (above the peak electron density), which are shown with red color dumbbells for more clarity. Figures 2a and 2b show near vertical and positive gradients at around 410-500 km and 460-500 km range, whereas Figure 2c shows both positive and near vertical at 300-400 km and 400-500 km range and Figure 2d shows positive gradient at 350-400 km and 450-500 km range. Though the shapes of density profiles are not intact in most of the profiles, it is nearly impossible to scale important ionosphere parameters of both bottomside and topside ionosphere from these unreliable and questionable density profiles.

3. CALCULATION OF MEAN DEVIATION AND TOPSIDE SLOPE OF DENSITY PROFILES

Rather than relying on any model and other observations, we set up the criteria of data quality control to remove unreliable and questionable data by using mean deviation (MD) of electron density fluctuations and slope (or vertical gradient) of the topside electron density profile as explained in the following lines.

The MD is defined as

$$MD = \sum_i \frac{\left| n_{ei} - \overline{n_{ei}} \right|}{N \overline{n_{ei}}} \quad \ldots (1)$$

where N is the total data point in a profile, n_{ei} and $\overline{n_{ei}}$ are, respectively, the measured and background (obtained by taking 9-point running average of the measured electron density

profile) electron densities at the i-th height. It is obvious from the equation (1) that the farther the measured electron density deviates from the background value, the larger the magnitude of MD will be. Statistics show majority of MDs appear in range between 0-1.5, therefore, we set up threshold level of 1.5 for the value of MD for screening-out the questionable and unreliable data. In addition, retrieved electron density profiles for the conditions of Kp index (a planetary geo-magnetic storm index) greater than 3 are also needed to be deleted if one wishes to limit effects from the geomagnetic disturbances. In this research, we have applied our approach to relinquish questionable as well as density profiles associated with Kp index greater than 3 and have made quantitative comparisons between the number of original and remaining density profiles.

Aside from the enormously large spikes, it is also true that a number of electron density profiles show positive gradient or nearly uniform distribution in the topside portion of the F-layer (above NmF2). As will be shown in the following lines, the topside slopes of density profiles are calculated by dividing the electron density profile with altitude in the height range between 420 and 490 km.

$$Slope = \left[(Ne_{490} - Ne_{420}) / (h_{490} - h_{420}) \right] \ldots (2)$$

Note that the calculated slope is similar to the altitude changing rate of electron density (Ne) i.e. dNe/dh, or simply gradient. Nevertheless, instead of considering next level of altitude that generally adopt in the calculation of dNe/dh, we consider the initial altitude at 420 km and final altitude at 490 km to calculate the topside slope in this research. After implementing our criteria of data quality control based on fluctuation and gradient of the topside density profile, around 65270 questionable electron density profiles were discarded from the total number of occultations 3337723 between July 2006 and May 2013 (83 months period), which is around 2%. Since we have also deleted density profiles that come under magnetically disturbed periods (i.e., Kp >3), which are nearly 516001 (~15%) profiles, discarded total profiles were around 581271 (~17%) during this 83 month period. Figure 3 shows the bar diagram of electron density raw profiles (blue bars) and remaining density profiles (snuff bars) after implementation of the so-called data quality control criteria along with Kp >3 condition,

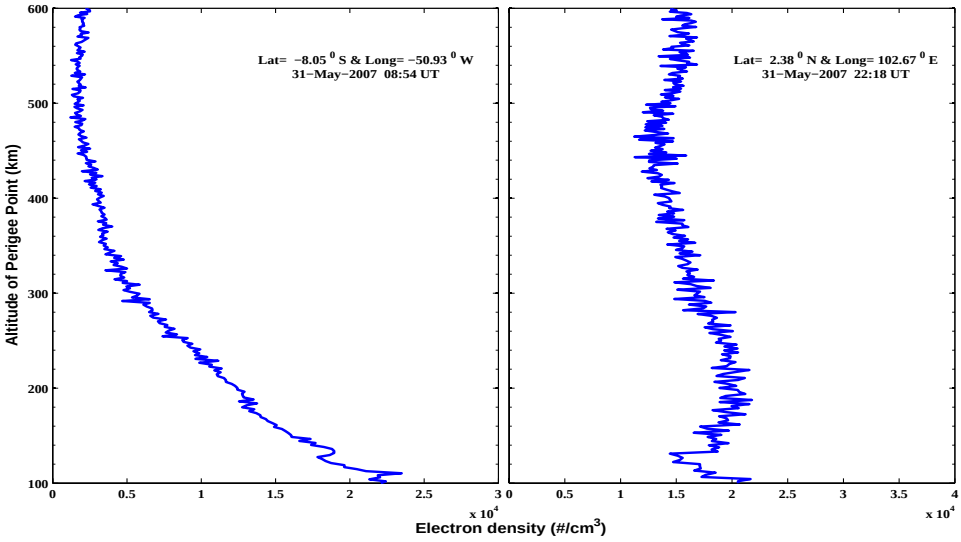

Figure 1 shows highly unreliable and questionable electron density profiles at southern (left) and northern (right) hemispheres retrieved by the COSMIC satellite (FM2) on 31 May 2007, in which scaling of ionospheric parameters is nearly impossible.

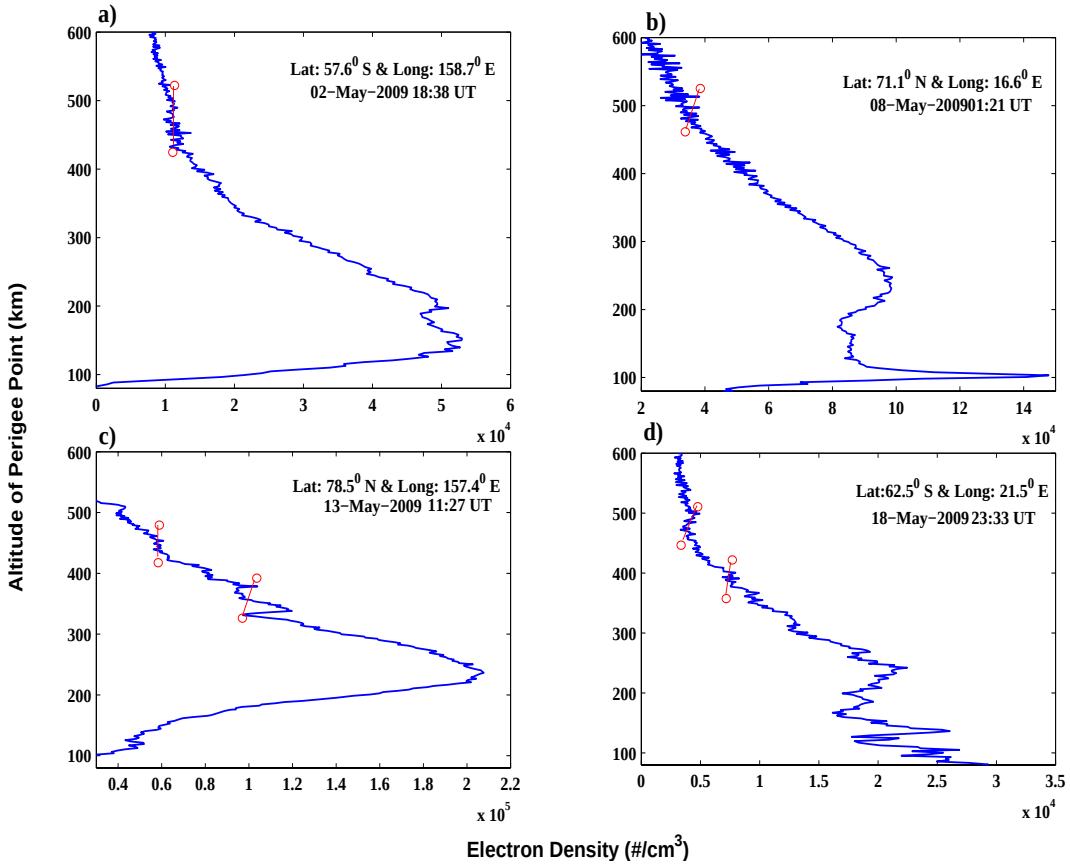

Figures 2a-2d show different COSMIC electron density profiles with positive slopes at the topside ionosphere that are marked with red color dumbbell.

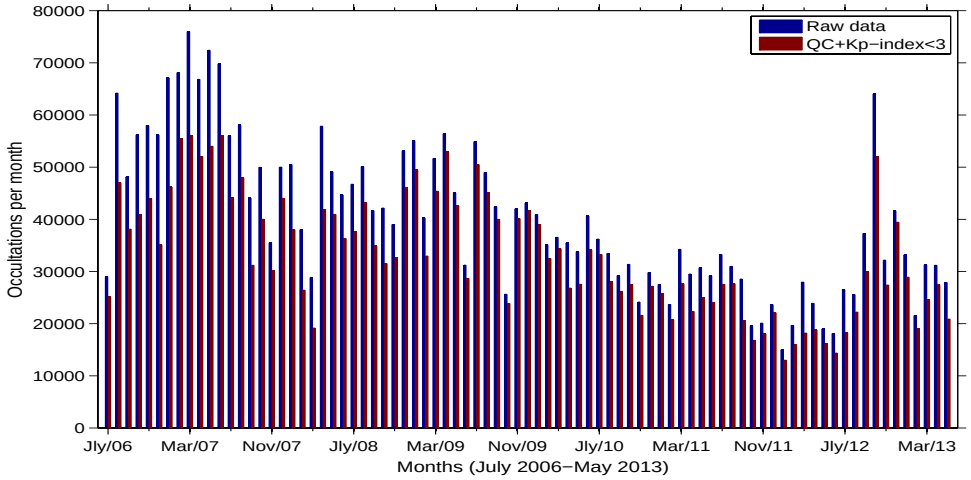

Figure 3 shows a bar graph, wherein the total number of COSMIC occultations before and after QC checks during July 2006 and May 2013 are presented

4. MEAN DEVIATIONS AND TOPSIDE IONOSPHERE SLOPES

Figure 4 depicts the global distributions of magnitudes of MDs in different seasons including March equinox (March, April and May), June solstice (June, July and August), September equinox (September, October and November), and December solstice (December, January and February) during 2007-2012, in which the geo-magnetic equator (red curve) is also shown. As indicated, the higher the latitude is, the larger the fluctuation in MDs will be. Although enormously large disturbances occur over the polar region where the latitude is greater than about 70°, the southern polar regions are associated with higher values during most of the seasons. This feature strongly suggests that the ionospheric electron densities in the southern polar region were much more irregular than those in the northern polar region. It is conceivable that the irregular fluctuation of the electron density profile is associated with ionospheric plasma irregularities that make the spherical symmetry invalid in the retrieval of the ionospheric refractive index from the bending angle of the GPS ray in accordance with Abel transformation.

A close look at this figure reveals particularly during different seasons of extreme LSA year (2008) that the northern hemisphere's polar region is associated with relatively lesser magnitudes. It may be worth mentioning here that the high latitudes were characterized with no scintillation activity that measured from the signal-to-noise ratio (SNR) intensity fluctuations of L1 channel of GPS radio occultation (RO) signals using COSMIC micro-satellites, possibly due to the absence of drives of instabilities in the auroral, cusp and polar cap regions, namely the gradient drift and velocity shear during an extreme LSA year 2008 [*Brahmanandam et al. 2012*]. Further, with the transition of solar activity from low, less than 100 solar flux units (SFU and 1 SFU = 10^{-22} W/m^2/Hz) between July 2006 and December 2010, to higher levels, greater than 100 SFU after January 2011, other regions of the globe are also showing higher MDs. This trend seems to be increasing with increasing solar activity, giving evidence that the MDs are showing solar activity dependent behavior.

The global trends of topside slopes as shown in Figure 5 are clearly showing a pronounced variation within around $\pm 40^0$ latitudes and no such features are found above around $\pm 40^0$ latitudes during most of the seasons. This feature clearly implying that the higher latitudes are associated with positive or nearly equal slopes irrespective of different solar activity years. In the similar lines with global MD trends, solar activity dependent is also evident for topside slopes, although no specific features are observed during an extremely LSA year 2008.

5. TYPICAL COMPARISONS

An attempt is made to cross-examine the above typical features between unprocessed and processed density profiles. Figure 6 depicts the global (geographic longitude vs. latitude) peak density variations of unprocessed (topside panels) and processed (bottomside panels) profiles during March-April 2009, in which the geomagnetic equator is shown with a thick red line. It is obvious that few differences are observed clearly between unprocessed and processed profiles during March 2009, particularly in EIA structure and magnitudes associated with them. For example, EIA structures over the entire Pacific Ocean regions are not appearing for unprocessed profiles and the magnitudes associated with EIA structures at west and east side of African continent, over the south American continents and over the eastern part of Indian ocean are not comparable with processed density profile during March 2009. Nevertheless, in general, a coherency in overall trend between unprocessed and processed profiles is found during most of the months (not shown). Figure 7 depicts the global (geographic longitude vs. latitude) peak height variations of unprocessed (topside panels) and processed (bottomside panels) profiles

during March-April 2009, in which the geomagnetic equator is shown with a thick red line. Unlike global peak densities, no prominent differences in peak heights are found between unprocessed and processed profiles.

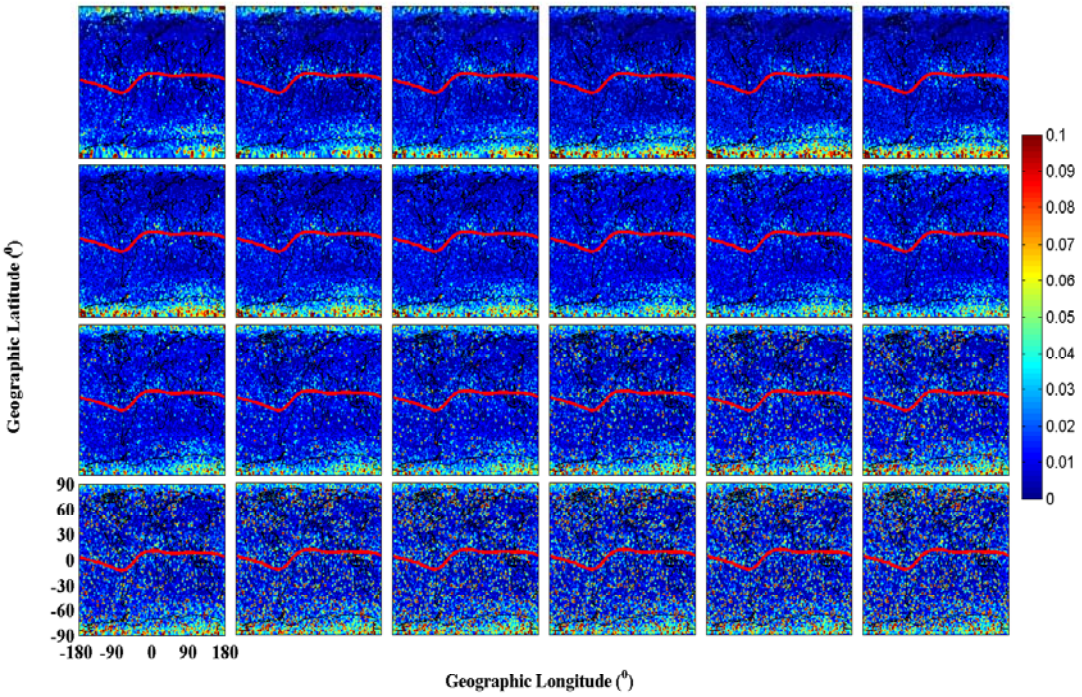

Figure 4 shows global-seasonal variations of mean deviations of processed density profiles during different seasons between 2007 and 2012

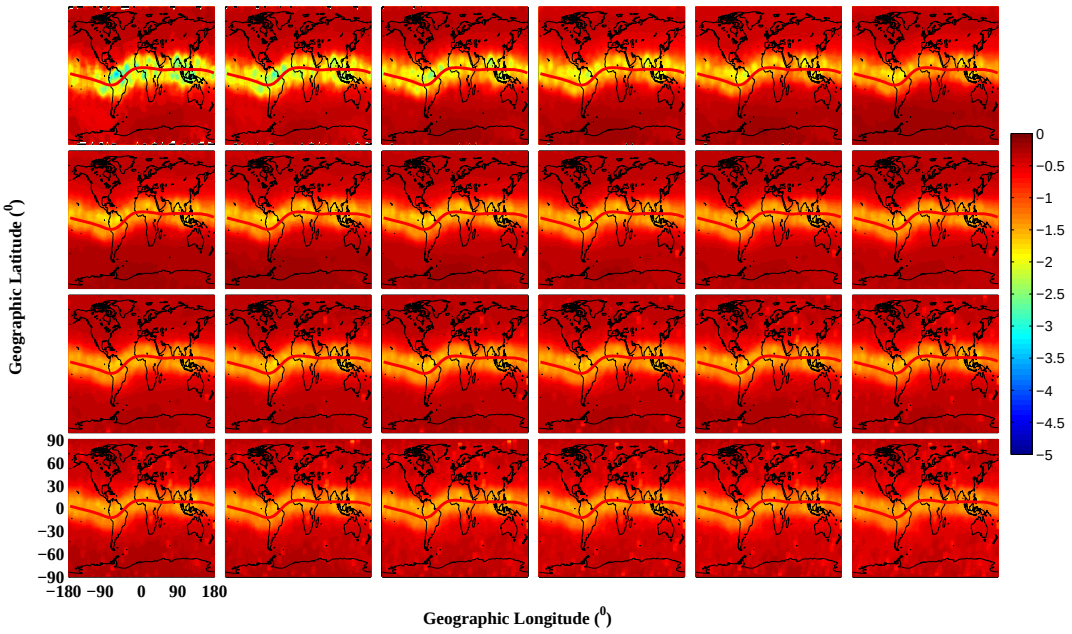

Figure 5 shows global-seasonal variations of topside slopes of processed density profiles during different seasons between 2007 and 2012

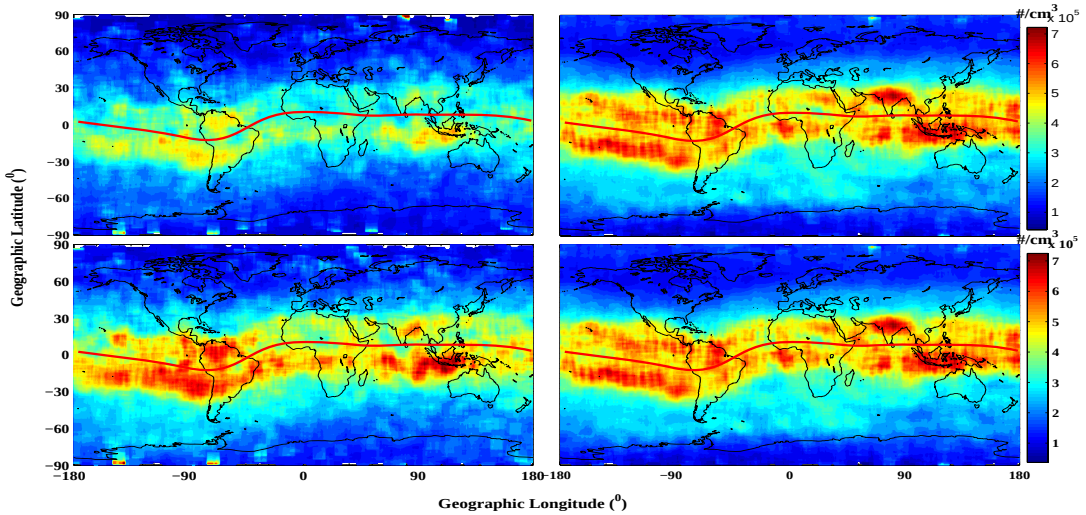

Figure 6 Global map of peak electron densities in March and April 2009 between raw (upper panels) and processed density profiles (lower panels)

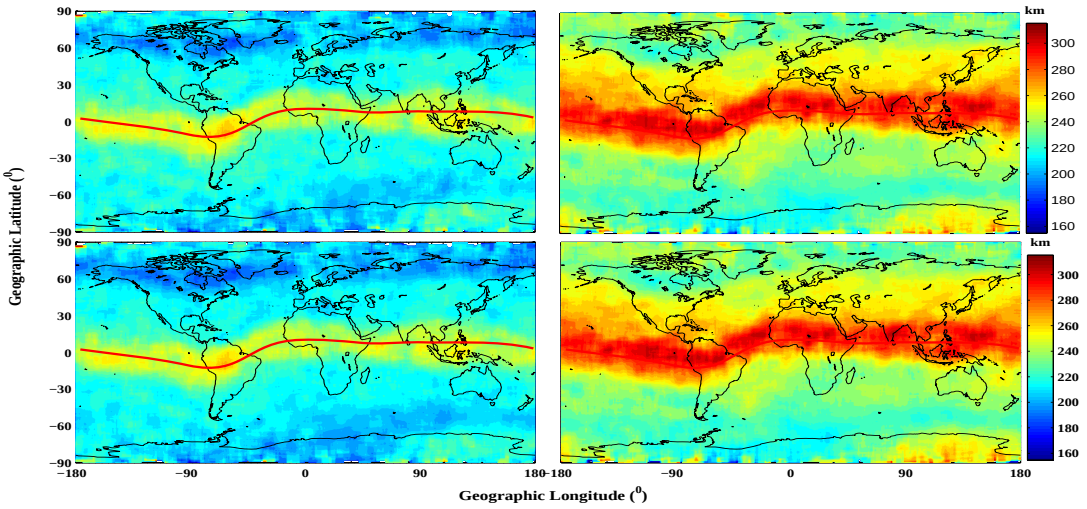

Figure 7 Global map of peak heights in March and April 2009 between raw (upper panels) and processed density profiles (lower panels).

N. CONCLUSIONS

After the implementation of this innovative data quality control scheme, more than 581271 (~17%) questionable profiles were discarded during the 83 months study period (July 2006-May 2013). The plotted global trends of mean deviations and topside fluctuations have shown solar activity dependency and pronounced variations between around $\pm 40^0$ latitudes. Importantly, a comparison of peak electron densities between unprocessed and processed density profiles has shown remarkable differences in large-scale structures and magnitudes associated with them, which indicating that the electron density profiles being provided by COSMIC RO technique need to be used only after the deletion of questionable profiles. Though CDAAC do not filter the so-called questionable electron density profiles at present, it is anticipating that such efforts will

be taken during its future missions such as COSMIC-2 which is going to be launched during the mid of 2016. However, in order to delete the so-called questionable profiles being provided by COSMIC RO technique our procedure may be helpful.

ACKNOWLEDGEMENTS

COSMIC data were obtained from the Taiwan Analysis Center for COSMIC (TACC)/COSMIC Data Analysis and Archive Centre (CDAAC). Authors would also like to acknowledge the management of Madanapalle Institute of Technology & Science (MITS), Madanapalle, AP, India for providing full logistical support to carry-out this present research.

REFERENCES

Brahmanandam, P. S., G. Uma, J. Y. Liu, et al., (2012), Global S4 index variations observed using FORMOSAT-3/COSMIC GPS RO technique during a solar minimum year. *J. Geophys. Res.*, 117, A09322, doi: 10.1029/2012JA017966.

Chu Y. H, C. L. Su, and H-T, Ko (2010), A global survey of COSMIC ionospheric peak electron density and its height: A comparison with ground-based ionosonde measurements, *Adv. Space Res.,* 46, 4, 431-439.

Hajj, G. A., L. C. Lee, X. Pi, L. J. Romans, W. S. Schreiner, P. R. Straus, and C. Wang (2000), COSMIC GPS ionospheric sensing and space weather. *Terr. Atmos. Oceanic Sci.,* 11, 235–272.

Kursinski, E. R., Hajj, G. A., Leroy, S. S., and Herman, B, (2000), The GPS radio occultation technique, *Terr. Atmos. Ocean. Sci.*, 11, 53–114.

Potula, B. S., Y.-H. Chu, G. Uma, H.-P. Hsia, and K.-H. Wu (2011), A global comparative study on the ionospheric measurements between COSMIC radio occultation technique and IRI model, *J. Geophys. Res.*, 116, A02310, doi:10.1029/2010JA015814.

Scherliess, L., and B. G. Fejer (1999), Radar and satellite global equatorial F region vertical drift model, *J. Geophys. Res.,* 104, 6829 – 6842, doi:10.1029/1999JA900025.

Yang, K. F., Y. H. Chu, C. L. Su, H. T. Ko, and C. Y. Wang (2009), An examination of FORMOSAT-3/COSMIC F peak measurements: Data quality criteria and comparisons with the IRI model, *Terr. Atmos. Ocean. Sci.,* 20, 193– 206, doi:10.3319.

Yue, X., Schreiner, W. S., Lei, J., Sokolovskiy, S. V., Rocken, C., Hunt, D. C., and Kuo, Y.-H (2010), Error analysis of Abel retrieved electron density profiles from radio occultation measurements, Ann. Geophys., 28, 217-222, doi:10.5194/angeo-28-217-2010.

Yue X, Schreiner W. S, Lin YC, Rocken C, Kuo YH, Zhao B (2011b), Data assimilation retrieval of electron density profiles from radio occultation measurements. *J Geophys Res*., 116:A03317. doi: 10.1029/2010JA015980

Yue, X., *et al. (*2013*),* The effect of solar radio bursts on the GNSS radio occultation signals*, J. Geophys. Res.,* 118, 5906–5918.